



Marian Klasztorny<sup>1\*</sup>, Daniel B. Nycz<sup>2</sup>, Kamil Zajac<sup>1</sup>, Roman K. Romanowski<sup>3</sup>

<sup>1</sup>Military University of Technology, Faculty of Mechanical Engineering, Department of Mechanics & Applied Computer Science, ul. gen. S. Kaliskiego 2, 00-908 Warsaw, Poland

<sup>2</sup>Institute of Technology, Jan Grodek State Vocational Academy, ul. W.S. Reymonta 6, 38-500 Sanok, Poland

<sup>3</sup>ROMA Co. Ltd., ul. Słoneczna 7, Grabowiec, PL-87124 Złotonia, Poland

\*Corresponding author. E-mail: m.klasztorny@gmail.com

Received (Otrzymano) 7.02.2017

## MODELLING AND NUMERICAL STUDY OF COMPOSITE SIDE SAFETY DEVICE FOR WIELTON TRUCKS

The numerical modelling and simulation of approval tests of a side safety device (anti-bicycle buffer) for Wielton trucks was developed. The new type of device is made of glass-reinforced polyester laminates, manufactured using press technology. As part of the design, simulation of approval tests of the new design solution was conducted for five variants of the composite shells using MSC.Marc finite element code. The results are presented in the form of deflection contour maps and equivalent effort index contour maps for the laminate shells. The load capacity and usability conditions with respect to the buffer were checked. It was shown that all the analysed options of the GFRP composite buffer fulfil the approval conditions. The buffer case, optimal in respect to structural materials and formation technology, was recommended for production. The simulation results of the approval tests on the deflections of the side safety device chosen for production were compared with the results of the experimental approval tests. Good qualitative and quantitative agreement of the results was observed.

**Keywords:** side safety device, glass-reinforced polyester laminate, modelling, numerical study, experimental verification

## MODELOWANIE I BADANIA NUMERYCZNE KOMPOZYTOWEGO BOCZNEGO URZĄDZENIA ZABEZPIECZAJĄCEGO DO POJAZDÓW CIĘŻAROWYCH WIELTON

Przeprowadzono modelowanie numeryczne i symulację testów homologacyjnych boczne urządzenie zabezpieczające (odboju antyrowerowego) do pojazdów ciężarowych Wielton. Urządzenie nowego typu jest wykonane z laminatu poliestrowo-szklanego. Do wytwarzania urządzenia zastosowano technologię prasowania. W ramach projektowania, przeprowadzono symulację testów homologacyjnych nowego rozwiązania konstrukcyjnego dla pięciu wariantów powłok kompozytowych. Zastosowano oprogramowanie MSC.Marc. Wyniki przedstawiono w formie map ugięć oraz map zastępczego indeksu wyężenia powłok laminatowych. Sprawdzono warunki nośności i użyteczności odboju. Wykazano, że wszystkie warianty odboju kompozytowego spełniają warunki homologacyjne. Do produkcji wybrano wariant optymalny pod względem materiałowo-technologicznym. Wyniki testów homologacyjnych w zakresie ugięć boczne urządzenie zabezpieczające wybranego do produkcji porównano z wynikami testów eksperymentalnych. Uzyskano dobrą zgodność jakościową i ilościową wyników testów symulacyjnych z wynikami testów eksperymentalnych.

**Słowa kluczowe:** boczne urządzenie zabezpieczające, laminat poliestrowo-szklany, modelowanie, badania numeryczne, weryfikacja eksperymentalna

## INTRODUCTION

A side safety device (assumed code SSD) on large vehicles is used to protect cyclists from falling under the vehicle in the event of an accident/collision. An SSD device, commonly called an anti-bicycle buffer, bumper or cover, is part of the equipment of trailers/semi-trailers of trucks. Most frequently, SSDs in the form of prismatic one- or two-box, thin-walled aluminium profiles are available on the market, for which individual screw connectors should be designed for a given trailer/semi-trailer. Galvanized steel covers and EPDM rubber overlays are also offered [1].

WIELTON J.-S. Co. ([www.wielton.com](http://www.wielton.com)), in collaboration with ROMA Co. Ltd. ([www.roma.torun.pl](http://www.roma.torun.pl)) and the Military University of Technology ([www.wat.edu.pl](http://www.wat.edu.pl)),

designed a new type of a GFRP composite SSD for Wielton trucks. The paper presents the numerical modelling and simulation of the approval tests on this device. Five options of GFRP composite shells are examined. For the laminate shells the numerical modelling and simulation methodology developed in [2] was applied.

## STRUCTURE AND FORMATION TECHNOLOGY WITH RESPECT TO SSD

A new SSD on the Wielton trailers/semi-trailers is a guard element made of GFRP composite, of an origi-

nal external industrial design owned by the WIELTON company (Fig. 1). On the rear side, a trapezoidal composite rib with PU foam core is designed, located on the section between the embossing patterns. Figure 1 shows the construction drawings of the SSD. From the front side, radiused surfaces and edges and round and elongated embossing patterns are applied. Screw connections reflecting hinged supports on the chassis longitudinal beam are used, i.e. two M8 screws on each support.

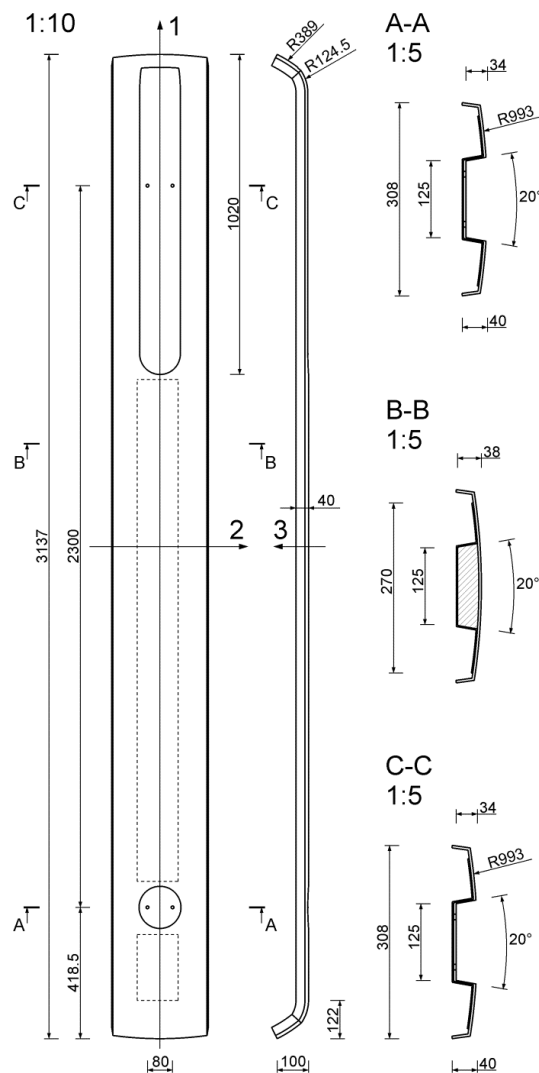


Fig. 1. Side safety device: front view, side view, cross sections

Rys. 1. Boczne urządzenie zabezpieczające: widok z przodu, widok z boku, przekroje poprzeczne

The design parameters are the ply sequences in the front and rear composite shells. The permissible total thickness of the buffer, specified by the truck manufacturer, is 40 mm. A trial series of SSD was produced by the ROMA company, specializing in modern technologies and the production of glass-reinforced composite structures.

The trial series was manufactured using press technology at 24°C. The concave ends of the foam core were cut using a CNC machine so that there were no clearances between the embossing patterns and the

core. The rigid closed mould consists of the bottom mould (in contact with the front side of the buffer) and the upper mould (in contact with the rear side of the buffer). After application of the release agent on the surfaces of the bottom and upper moulds, a decorative layer is spread in the bottom mould as a gelcoat layer with anti-osmosis properties and improved flexibility and mechanical strength. Glass reinforcement layers forming the front shell, foam core and glass reinforcement forming the rear shell are put on the gelcoat layer. Subsequent reinforcement layers, respectively stacked due to the embossing, are initially supersaturated with polyester resin. Closing the mould using a press is followed by supersaturation of the glass reinforcement, squeezing out the excess resin, gelation and curing the resin.

## NUMERICAL MODELLING OF SSD AND DESCRIPTION OF APPROVAL TESTS

A geometric model of the buffer was made using Catia v5 software. Simplification of the geometry to the middle surfaces and finite element (FE) meshing of the model were performed using the Altair HyperMesh v12.0 programme. An average size of FE mesh of 10 mm was used. Figure 2 shows the geometric model of the buffer from the front view, overlaid with the FE mesh. The modelling omitted relatively soft foam filling which is only for technological purposes, and only serves to produce the trapezoidal rear rib.

The finite elements of QUAD4 (15841 FEs) and TRIA 3 (22 FEs) topology are assigned to the Bilinear Thick-shell Element formulation [3]. The material model for the laminate layers is assumed as an orthotropic, linear, elastic-brittle model with Hashin Fabric progressive failure criterion [4].

The material constants of the laminae are summarized in Table 1 [2]. Directions 1, 2 coincide with the warp and weft fibre directions, respectively, and direction 3 is the direction of thickness of the laminae. 1 is the direction parallel to the buffer axis, 2 is the direction orthogonal to 1, and 3 corresponds to the direction of horizontal deflections of the buffer mounted on the vehicle. Table 1 summarizes the following material constants:

$E_1, E_2$  - Young's modules in directions 1, 2

$\nu_{12}$  - Poisson's ratio in plane 12

$G_{12}, G_{13}, G_{23}$  - shear modules in planes 12, 13, 23

$R_{1t}, R_{1c}, R_{2t}, R_{2c}$  - tensile strength and compressive strength in directions 1, 2

$R_{12}, R_{13}, R_{23}$  - shear strengths in planes 12, 13, 23.

The above mentioned material constants describe the material model adopted in the numerical calculations. Code FRC indicates a composite reinforced with a plain weave glass fabric, and code MRC indicates a composite reinforced with a glass mat. The modelling assumed thicknesses of the laminate obtained using hand lay-up technology, since the material constants

were identified using samples cut from plates produced using this technology, i.e. 0.70, 0.95, 1.10, and 1.60 mm respectively for a mat weighing 300 g/m<sup>2</sup> and fabrics weighing 450, 600, 800 g/m<sup>2</sup>. Press technology results in reducing the thicknesses of the laminae and increasing the reinforcement volumetric fraction. The influence of the resin mass reduction on the deflections and failure indices of the GFRP composite buffer was neglected.

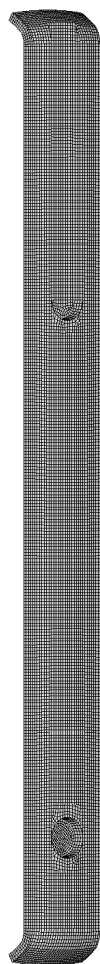


Fig. 2. Numerical model of SSD (FE mesh) - front view

Rys. 2. Model numeryczny SSD (siatka elementów skończonych) - widok z przodu

TABLE 1. Elastic and strength constants of glass-polyester composites (FRC - fabric reinforced composite, MRC - mat reinforced composite)

TABELA 1. Stałe sprężystości i wytrzymałości kompozytów poliestrowo-szklanych (FRC - kompozyt wzmocniony tkaniną, MRC - kompozyt wzmocniony matą)

Constant	Unit	FRC	MRC
$E_1, E_2$	[GPa]	17.7	8.94
$\nu_{12}$	-	0.15	0.40
$G_{12}$	[GPa]	2.43	2.79
$G_{13}, G_{23}$	[GPa]	0.564	0.989
$R_{1t}, R_{2t}$	[MPa]	279	99.0
$R_{1c}, R_{2c}$	[MPa]	203	221
$R_{12}$	[MPa]	34.5	87.9
$R_{13}, R_{23}$	[MPa]	23.0	34.7

The design solution of the SSD is a simply supported beam with two cantilevers. M8 screw connections were used, implementing hinged supports unmovable lengthwise on the first support and sliding longitudinally on the second support. Such a beam corresponds to two approval tests shown in Figure 3 [5]. The buffer beam has to transfer without damage the load in the form of a concentrated force of 1 kN, applied perpendicularly to the front surface in the middle position and in the end position on the side with the elongated embossing. The load is applied by a cylindrical punch having a diameter of 220 mm±10 mm. The beam deflection limit,  $w_p$ , under the centre of the stamp is 150 mm in the case of the load in the middle position and 30 mm in the case of the load in the end position. The equivalent effort index limit for the laminate shells was adopted,  $R_p = 0.60$  [2].

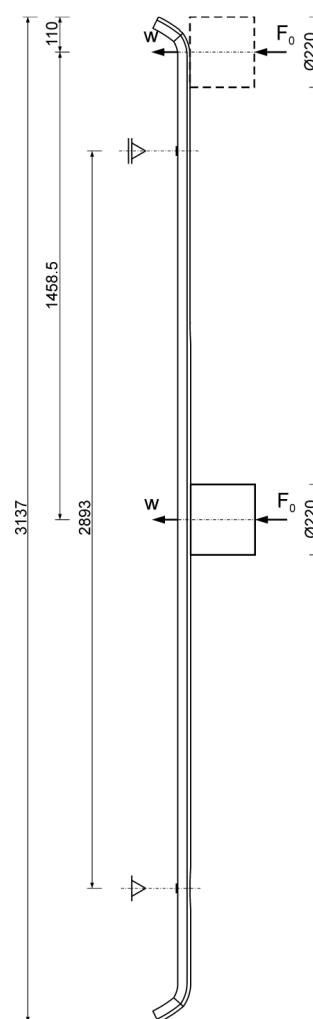


Fig. 3. Approval test loads for SSD: middle load (solid line), end load on side with elongated embossing (broken line)

Rys. 3. Obciążenia testowe homologacyjne SSD: obciążenie środkowe (linia ciągła), obciążenie skrajne od strony wytłoczenia podłużnego (linia przerywana)

The equivalent effort index corresponding to the Hashin fabric failure criterion and FEs in the Bilinear Thick-shell Element formulation is defined as follows [2-4]:

$$R = \max(R_i), \quad i = 1, 2, 3, 4 \quad (1)$$

where

$$R_i = \sqrt{F_i} \quad i = 1, 2, 3, 4 \quad (2)$$

are the effort indices respectively assigned to the following failure indices:

$$F_1 = \left[ \left( \frac{\sigma_1}{R_{1t}} \right)^2 + \left( \frac{\sigma_{12}}{R_{12}} \right)^2 + \left( \frac{\sigma_{13}}{R_{13}} \right)^2 \right], \quad \text{at } \sigma_1 > 0$$

$$F_2 = \left[ \left( \frac{\sigma_1}{R_{1c}} \right)^2 + \left( \frac{\sigma_{12}}{R_{12}} \right)^2 + \left( \frac{\sigma_{13}}{R_{13}} \right)^2 \right], \quad \text{at } \sigma_1 < 0$$

$$F_3 = \left[ \left( \frac{\sigma_2}{R_{2t}} \right)^2 + \left( \frac{\sigma_{12}}{R_{12}} \right)^2 + \left( \frac{\sigma_{23}}{R_{23}} \right)^2 \right], \quad \text{at } \sigma_2 > 0$$

$$F_4 = \left[ \left( \frac{\sigma_2}{R_{2c}} \right)^2 + \left( \frac{\sigma_{12}}{R_{12}} \right)^2 + \left( \frac{\sigma_{23}}{R_{23}} \right)^2 \right], \quad \text{at } \sigma_2 < 0 \quad (3)$$

In Equations (3), quantities  $\sigma_1, \sigma_2$  are normal stresses in directions 1, 2, and  $\sigma_{12}, \sigma_{13}, \sigma_{23}$  are shear stresses in the orthotropic planes 12, 13, 23, respectively. For shell FEs the remaining failure indices,  $F_5, F_6$ , vanish. The buffer was loaded using a perfectly rigid cylindrical punch with a diameter of 220 mm, applying forced excitation in the two variants shown in Figure 3. Between the punch and the buffer, the Touching contact model was adopted based on the constrain method [4]. For the composite-steel friction pair, the Coulomb friction coefficient was equal to 0.29 [6].

## SIMULATION RESULTS FOR APPROVAL TESTS OF SSD

Simulations of the approval tests of the SSD beam were performed for the five variants of the ply sequences of the front and rear laminate shells, listed in Table 2. Codes STR, EM indicate quasi-balanced plain weave glass fabrics and a glass mat, respectively. They are glass products produced by KROSSLASS J.-S. Co., Krosno, Poland.

TABLE 2. Tested ply sequences of laminate shells  
TABELA 2. Sekwencje warstw powłok laminatowych objęte symulacją

Ply sequence	Front laminate Rear laminate
S1	EM300/STR800/STR800/STR800 STR800/STR800/STR800
S2	EM300/STR800/STR800 STR800/STR800
S3	EM300/STR800 STR800
S4	EM300/STR600/STR600 STR600/STR600
S5	EM300/STR450/STR450 STR450/STR450

The numbers following codes STR or EM reflect the weight per unit area [ $\text{g}/\text{m}^2$ ]. The static calculations of the SSD beam were carried out using MSC.Marc FE code and the Newton-Raphson method with force and displacement convergence criteria [2].

The simulation results are shown in a graphical form for the S1, S5 extreme cases. Figure 4 shows the contour maps of the deflections in the load direction and deformation of the SSD (scale 5:1) for sequence S1. Figure 5 presents the contour maps of the equivalent effort index,  $R$ , including all the laminate layers and the first four failure indices of the Hashin Fabric criterion for sequence S1. Analogous results for sequence S5 are shown in Figures 6 and 7.

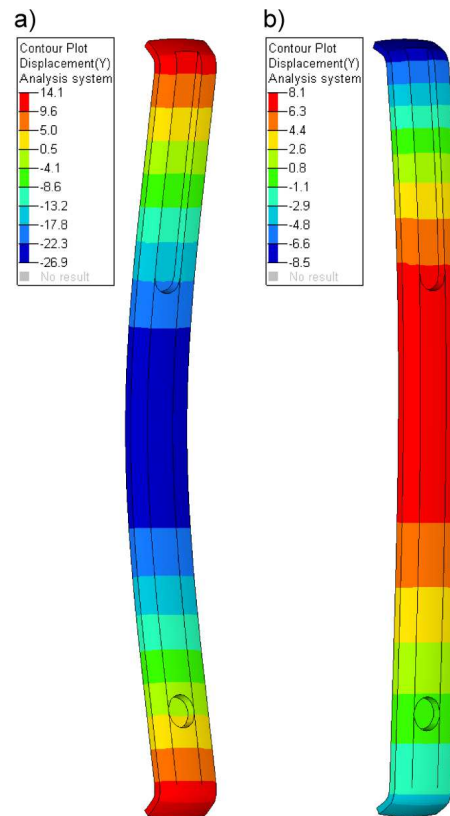


Fig. 4. Deflection contour map and deformation for SSD beam with ply sequence S1 (deformation scale 5:1): a) middle load, b) end load

Rys. 4. Mapa warstwowa ugięć i deformacja belki SSD z sekwencją S1 (skala deformacji 5:1): a) obciążenie środkowe, b) obciążenie skrajne

Deformations of the SSD beam are in line with the static scheme of a simply supported beam with cantilevers, loaded in the mid-span or at the end of the bracket. The equivalent effort index maps also correspond to this static scheme of the SSD. The maximum effort on the contact edges of the rigid stamp with the front composite shell and local stress concentrations around the bolts on the beam supports are visible. Table 3 compares the simulation deflection values of the buffer under the load-stamp in the middle and extreme positions and the simulation equivalent effort index values corresponding to five variants of the ply sequences in the front and rear laminate shells.

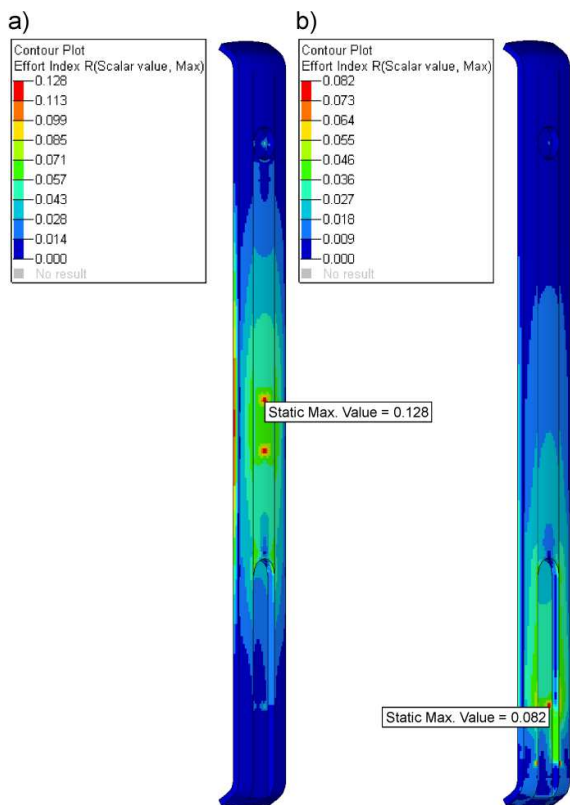


Fig. 5. Contour map of equivalent effort index  $R$  of SSD beam with ply sequence S1: a) middle load, b) end load

Rys. 5. Mapa warstwicowa zastępczego indeksu wyężenia  $R$  belki SSD z sekwencją S1: a) obciążenie środkowe, b) obciążenie skrajne

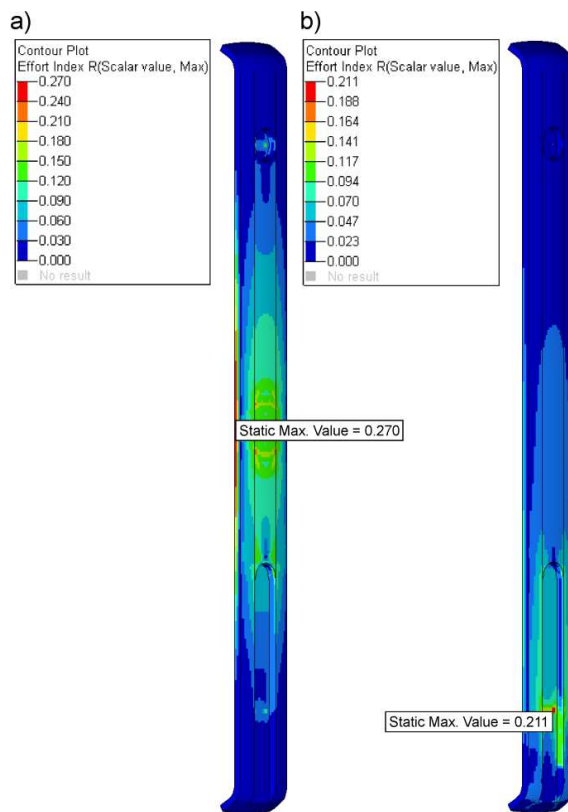


Fig. 7. Contour map of equivalent effort index  $R$  of SSD beam with ply sequence S5: a) middle load, b) end load

Rys. 7. Mapa warstwicowa zastępczego indeksu wyężenia  $R$  belki SSD z sekwencją S5: a) obciążenie środkowe, b) obciążenie skrajne

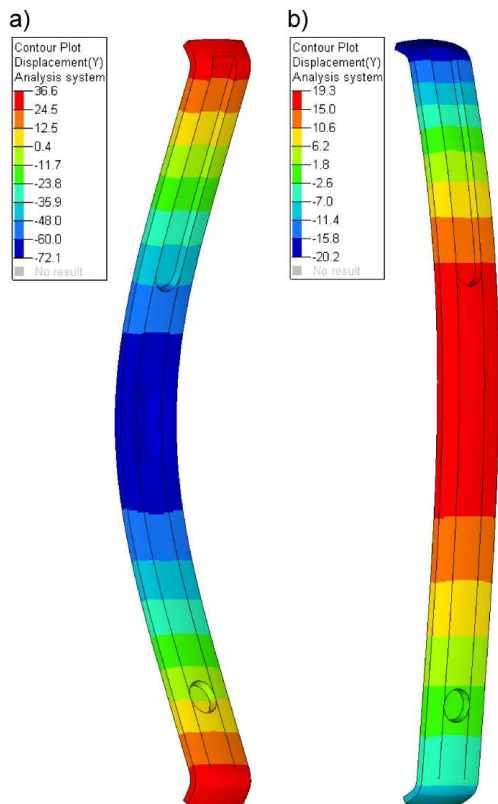


Fig. 6. Deflection contour map and deformation for SSD beam with ply sequence S5 (deformation scale 5:1): a) middle load, b) end load

Rys. 6. Mapa warstwicowa ugięć i deformacja belki SSD z sekwencją S5 (skala deformacji 5:1): a) obciążenie środkowe, b) obciążenie skrajne

TABLE 3. Simulation values of deflection and equivalent effort index ( $R_p = 0.60$ ) for SSD

TABELA 3. Symulacyjne wartości ugięcia oraz zastępczego indeksu wyężenia ( $R_p = 0.60$ ) dla bocznego urządzenia zabezpieczającego

Ply sequence	Stamp position	$w_p$ [mm]	$w$ [mm]	$R$ [-]
S1	middle	150	26.8	0.13
	end	30	5.6	0.08
S2	middle	150	41.3	0.16
	end	30	7.5	0.12
S3	middle	150	87.5	0.33
	end	30	14.4	0.27
S4	middle	150	61.4	0.23
	end	30	10.4	0.18
S5	middle	150	71.7	0.27
	end	30	12.0	0.21

The experimental approval tests of the SSD beam in the S5 variant were performed in the Laboratory of the WIELTON company. The beams produced by the ROMA company had a 2.0 mm thick front laminate (average value including gelcoat) and 1.3 mm thick rear laminate. The test stand consisted of the following sub-systems: cylindrical weight of 100 kg and base diameter of 220 mm, SSD beam (buffer), supports and rigid elements replacing the main beam of the chassis. The SSD beam behaved linearly elastic. After removing the load, there was no mechanical damage in the laminate shells.

The simulation and experimental results regarding deflection are compared in Table 4. When the cylindrical weight is in the middle position, the simulation deflection is ~9% higher than in the experiment. When the cylindrical weight is in the end position on the side with the elongated embossing, the simulation deflection is ~14% lower than in the experiment. The experimental verification of the simulation tests was rated positively.

TABLE 4. Deflection of SSD beam with ply sequence S5 under stamp in simulation and experiment

TABELA 4. Ugięcia belki BUZ z sekwencją S5 pod stemplem, w symulacji i w eksperymencie

Stamp position	Deflection w [mm]	
	simulation	experiment
middle	71.7	66
end	12.0	14

## CONCLUSIONS

All the tested variants of the laminate shells (ply sequences S1, S2, S3, S4, S5) comply with the load capacity and usability conditions defined in the Regulations [5] and supplemented in this work. The SSD beam with ply sequence S5 was recommended for production. This sequence is characterized by the low glass reinforcement mass and good layering of the reinforcement on the embossing patterns. Compared with existing solutions, the recommended structural solution of SSD

can be competitive on the market due to the following advantages: relatively low weight (segment weight 9 kg) and corrosion resistance (no corrosion of the polymer matrix, high resistance to vibration protecting against micro crack initiation).

## Acknowledgements

*The work was done in the year 2016 within the framework of the statutory research project of the Department of Mechanics and Applied Computer Science, Faculty of Mechanical Engineering, Military University of Technology, Warsaw, Poland.*

## REFERENCES

- [1] [www.autoakcesoria.com.pl/sklep/zderzaki](http://www.autoakcesoria.com.pl/sklep/zderzaki). Uploaded 10/04/2016.
- [2] Klasztorny M., Nycz D., Cedrowski M., Modelling, simulation and validation of bending test of box segment formed as two composite shells glued together, *Composites Theory and Practice* 2015, 15(2), 88-94.
- [3] Marc 2008 r1, Vol. B. Element Library. MSC.Software Co., Santa Ana, CA, USA.
- [4] Marc 2008 r1, Vol. A. Theory and User Information. MSC.Software Co., Santa Ana, CA, USA.
- [5] Regulation No. 73 of the European Economic Commission of the United Nations - Uniform provisions concerning approval (in Polish), 9 Dec. 2010.
- [6] Nycz D.B., Modelling and numerical study of crash tests of barrier of class N2-W4-A on road arcs (in Polish), Military Univ. Technol. Press, Warsaw 2015.